Propellants, Explos., Pyrotech.

WILEY-VCH

Propellants, Explosives, Pyrotechnics

RESEARCH ARTICLE OPEN ACCESS

Investigation of Laser Initiation of Graphite-Coated TATP and HMTD with Regard to the Influence of Coating Thickness Accompanied by Sensor-Safe Surveillance Using a Microphone

Emre Ünal[1] | Matthias Muhr[1] | Thomas M. Klapötke[2] | Peter Kaul[1]

[1]Institute for Safety and Security Research, University Bonn-Rhein-Sieg, Rheinbach, NRW, Germany | [2]Faculty for Chemistry and Pharmacy, Ludwig-Maximilians Universität, Munic, BY, Germany

Correspondence: Emre Ünal (emre.uenal@h-brs.de) | Matthias Muhr (matthias.muhr@h-brs.de) | Peter Kaul (peter.kaul@h-brs.de) | Thomas M. Klapötke (tmk@cup.uni-muenchen.de)

Received: 25 June 2024 | **Revised:** 9 October 2024 | **Accepted:** 10 October 2024

Keywords: detection | laser initiation | multivariate statistics | primary explosives

ABSTRACT

Triacetone triperoxide (TATP) and Hexamethylene triperoxide diamine (HMTD), known for their propensity towards use in improvised explosive devices due to facile synthesis from readily accessible precursors, present a considerable security challenge. Their sensitivity to mechanical stimuli, such as impact and friction, as well as to thermal input, necessitates the development of advanced detection methodologies. This study is dedicated to evaluate the influence of varied laser beam parameters during radiation on these peroxide-based energetic materials. A novel approach for the controlled energy delivery to substances under investigation involves the application of coatings with predefined absorption coefficients. This technique, coupled with the careful selection of laser parameters, enables the controlled local initiation of reaction in the energetic material without reaching the threshold for mass combustion, thereby avoiding detonation or deflagration. The experimental setup involves the laser irradiation of defined quantities of graphite-coated TATP and HMTD, with the subsequent laser processing being monitored using a sensitive microphone. This set-up enables a detailed investigation of the physical phenomena that manifest themselves during the interaction and thus contributes to the state of knowledge about the safe handling and detection of these energetic materials.

1 | Introduction

Triacetone triperoxide (TATP) and Hexamethylene triperoxide diamine (HMTD) are highly dangerous explosives due to their extreme sensitivity to accidental ignition and propensity for spontaneous detonation [1, 2]. Their acute sensitivity to accidental ignition and likelihood of spontaneous detonation make them especially challenging to handle and detect safely [3–7]. The simplicity of their synthesis and the accessibility of their reactants have made them explosives of choice among terrorist groups, posing significant challenges to civil security [8–11]. Unlike many explosives, TATP and HMTD lack metallic elements and nitro groups, which complicates their detection through traditional spectroscopic techniques [12]. Consequently, non-destructive detection methods, especially those that do not require mechanical sampling, are preferred for identifying these materials. Techniques such as Raman spectroscopy, supported by laser technology, have achieved notable success in this area [13, 14]. Furthermore, approaches from the combination of microphone and the detection of explosives and vapours by means of acoustical spectroscopy have been tested and have produced promising results [15, 16]. Furthermore, the exploration of laser initiation of these explosives, aiming for a brief ignition time, has been a focus of research [17]. However, the use of laser radiation for the local and controlled initiation of energetic materials presents challenges, especially with primary explosives that have relatively low ignition thresholds and are likely to undergo complete combustion [15]. The application of coatings in laser processing has been studied to reduce the energy required for desired effects [18]. This approach involves coating substances with materials that possess a significantly higher absorption coefficient than the explosives themselves. The goal is to identify laser parameters and conditions that prevent the combustion of the entire explosive mass, especially with highly sensitive substances, while simultaneously initiating non-critical quantities, such as individual crystals. In this study, TATP and HMTD were synthesized and exposed to photonic radiation at power levels from 12.5 mW to 100 mW. The effect of graphite coatings of varying thicknesses on the processing and decomposition of these substances was investigated. Raman spectroscopy assessed the purity of the substances, while a microphone served as a reliable sensor for detecting partial conversions. This research aims to explore the behavior of TATP and HMTD under photonic irradiation, the impact of graphite coating on their decomposition, and how these coatings facilitate partial reactions at lower power levels.

2 | Experimental

2.1 | Synthesis of TATP

Caution. TATP is a strong explosive compound and requires experienced personnel. The synthesis was carried out according to Oxley et al. [19] Hydrogen peroxide at a concentration of 30% was carefully added to a reaction vessel. The vessel was then sealed with parafilm to prevent any contamination or evaporation and placed in an ice bath to keep the reaction temperature low. Anhydrous acetone was then added to the vessel containing the hydrogen peroxide solution. The components were stirred for at least 15 minutes to ensure good mixing. Concentrated sulphuric acid was then gradually added to the homogeneous solution. The mixture was left undisturbed for 24 hours at a reduced temperature. The reaction mixture was purified with methanol to remove DADP. The final product was then rinsed with distilled water to remove any remaining impurities.

2.2 | Synthesis of HMTD

Caution. HMTD is a strong explosive compound and requires experienced personnel. For the synthesis, hexamine was to an aqueous solution of formaldehyde in an ice bath. Subsequently, a hydrogen peroxide solution was gradually added. The reaction mixture was further treated by addition of citric acid. Precipitation of HMTD was observed within two hours, a significant reduction from the 5–6 hours normally required in the absence of formaldehyde. The reaction was allowed to run overnight while the temperature of the ice bath gradually increased to room temperature. The crude HMTD product was isolated by vacuum filtration, washed with distilled water to remove residual acid and then washed methanol to facilitate drying. The product was dried at room temperature [20, 21].

2.3 | Sample Preparation

Ahead of conducting the experimental measurements, the prepared samples were placed in a climate chamber and left undisturbed for a minimum duration of 48 hours at a controlled relative humidity of 20% and a temperature of 18°C. In the experimental setup, each specimen was placed into cylindrical metallic tubes with a diameter of 2 mm. The tubes were filled to a height of 5 mm and gently pressed manually with a suitable metal rod, which corresponds to an approximate sample mass of 10 mg. This type of sample preparation creates a surface that is not microscopically planar, which can increase the variability of the results. After filling, the samples were carefully sealed. For the preparation of coated samples, a mono or bilayer graphite deposition was executed, ensuring the complete drying of the initial layer prior to the application of the subsequent one. The graphite layers were administered using an aerosolised delivery method, facilitated by an airbrush apparatus positioned at a fixed distance of 10 cm from the target, with a spray exposure time precisely controlled at 500 ms. The particle size of the graphot was between 1 and 10 μm. Figure 1 shows specimens that have been prepared exemplary. A is an uncoated sample, B is a single-coated sample and C is a double-coated sample. In the following, samples are mostly labelled with abbreviations. oG stands for uncoated, mG for single-coated and 2mG for double-coated. The power and the consecutive number of the parameter set are given below. For example, TATP_mg_50 mW_2 is the second measurement of single-coated TATP and a power of 50 mW.

2.4 | Analytical Methods

2.4.1 | RAMAN

Samples were analysed for purity and the presence of by-products by Raman spectroscopy using a First Defender R by Thermo Fischer. The measurements were performed according to the standard operating procedures of the instrument. The spectral data subsequently obtained were compared to the instrument's inbuilt chemical library and analysed for confirmation.

2.4.2 | Microphone

During laser processing experiments, acoustic monitoring was carried out using a MEMS microphone (ELV MEMS1). Output voltage was captured via a DAQ card (Meilhaus Redlab FS 1208) set to a sampling 10 kHz.

2.4.3 | Laser

For the experiments, the samples were irradiated with a laser contructed by Laser Zentrum Hannover e.V. The laser used is

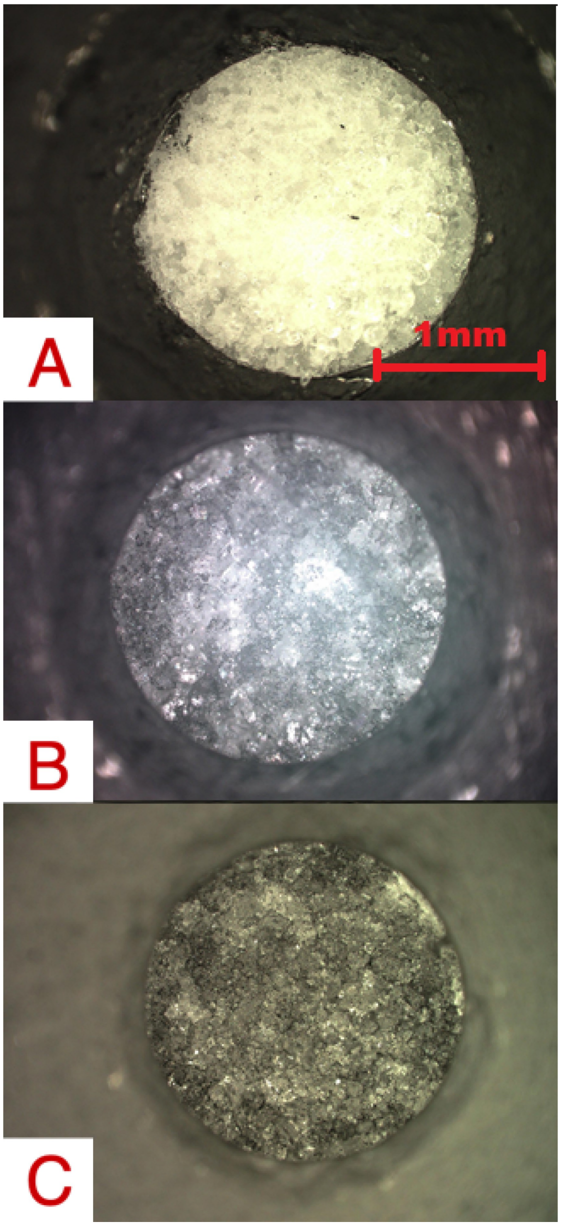

FIGURE 1 | Preparation and coating of TATP samples (magnification: 100x): A: uncoated, B: single-coated, C: double-coated.

a pulsed neodymium-doped yttrium aluminium doped laser (NdYAG). Its output wavelength is converted to 532 nm using a conversion crystal. The system has a maximum output power of 5 W and a pulse frequency of 2000 Hz. Each burst consists of exactly 10 pulses with a single-pulse energy of 2.5 mJ, with each pulse having a duration of 10 nanoseconds. A converging lens with a focal length of 250 mm is integrated into the system to refine and concentrate the optical power. A polarisation filter is used to precisely adjust the laser power. The power was checked using a power meter. The power fluctuations during adjustment are around ± 1 mW. The optical power and fluctuations were checked using a power meter in a time interval of about 1 min. The regulation of the irradiation was precisely controlled with the aid of a shutter programmed for an exposure time of 15 seconds per measurement cycle.

2.5 | Experiments

TATP and HMTD samples were investigated. These were each coated with graphite a different number of times and irradiated with the laser at different laser power and constant irradiation time. The basic influence of the graphite coating was analysed in order to be able to make a comparison with inert and explosive materials. As an organic reference material, sugar, also coated and uncoated, was analysed in the same structure and with the same parameters. All samples were irradiated with 12.5, 25, 50 and 100 mW for 15 s each at a distance of about 20 mm from the focus. The focus was located behind the sample so that the laser spot was defocused on the surface to a ratio of 500 μm. With the exception of HMTD, all tests were repeated three times. A schematic sketch of the structure is shown in Figure 2. Measurements with HMTD with two graphite layers and power $> = 50$ mW and TATP with power of 100 mW were omitted, as this always led to complete combustion of the sample. Data acquisition was performed using a DAQ card with a sampling 10 kHz, followed by moving average and envelope smoothing which is explained in detail in 2.6.

2.6 | Preprocessing

The preprocessing script for analogue microphone data involves cleaning the data by subtracting the mean of the first 1000 points to remove baseline drift and taking the absolute value to ensure all positive values [22]. An upper envelope is created by applying a rolling maximum over 1000 points, which highlights the data peaks and smooths short-term fluctuations. Subsequently, a rolling mean is calculated over 100 points to further smooth the data, followed by down-sampling to reduce data size and emphasize overall trends. These steps ensure the data are clean, smooth, and ready for accurate analysis by reducing noise and highlighting key features.

3 | Results and Discussion

3.1 | Raman Measurements

The spectra were acquired using the integrated software of the employed device and plotted against existing reference spectra. The spectra confirm that the substances used are indeed TATP and HMTD, with no significant impurities or competing products detected.

3.2 | Microphone Measurements

The data recorded by the microphone are discussed below. The presented plots are representative and illustrate the trends observed for each substance. The voltage output from the microphone was captured, and the following plots display measurements for each substance at a specific power level with all coating variations. To facilitate data analysis, pre-processing was conducted. Specifically, the absolute values of the signals

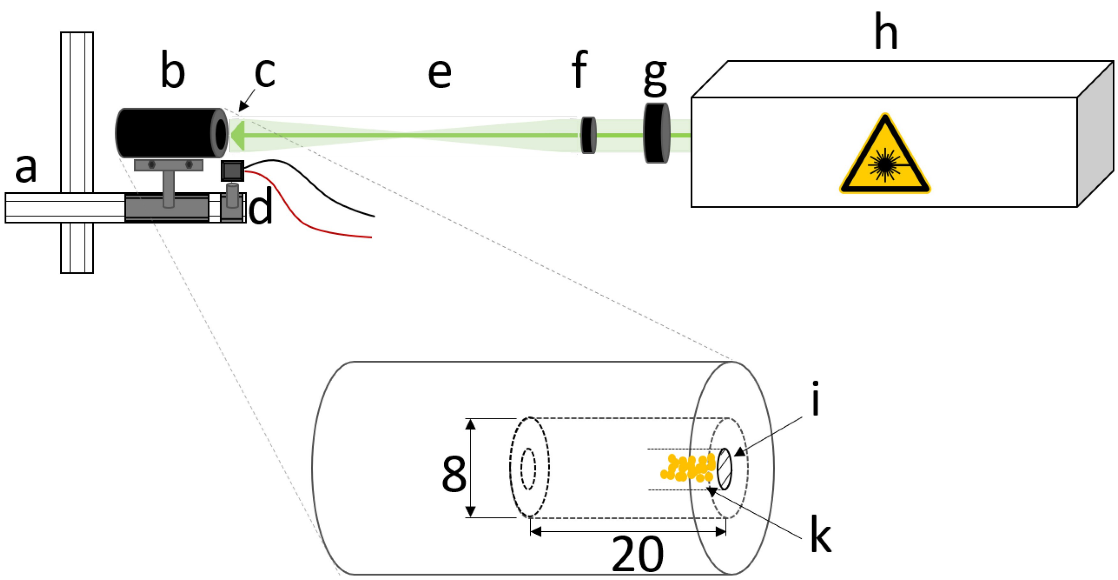

FIGURE 2 | Schematic sketch of the set-up -a: x-y stage, b: sample container, c: sample, d: microphone, e: laser beam, f: converging lens, g: shutter, h: laser system, i: sample container; coating (enlarged), k: sample (enlarged).

were utilized, as a significant signal can be identified at the start of each plot.

3.2.1 | Data Discussion

The following section presents and discusses the preprocessing voltage output of the microphone from measurements with varying coating and power. Measurements with HMTD with two graphite layers and power $>=50$ mW and TATP with power of 100 mW were omitted, as this always led to complete combustion of the sample.

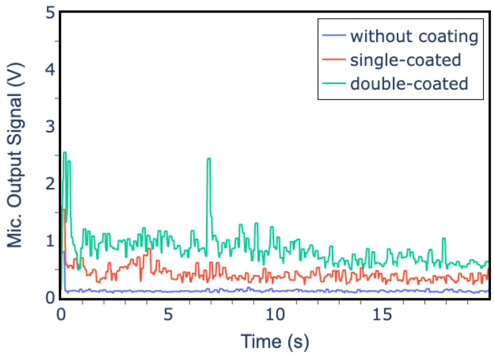

FIGURE 3 | Exemplary preprocessed microphone data of HMTD – 25 mW – all coatings.

Figure 3 shows the test results for a laser power of 25 mW and all three coatings as examples of HMTD measurements. At the beginning of each graph, a strong high signal can be seen, caused by the first impact of the laserbeam on the sample. This can be observed in all measurements and is generally stronger the higher the laser power. For the measurement without graphite coating, the microphone signal is around 0.8 V (Figure 3). Subsequently, a low, noisy signal can be recognised, which indicates a low level of processing (interaction of the laserbeam and the investigated material). There is no significant variation in intensity over time. The signal does not exceed 0.2 V after the laser has been applied for the first time. The exemplary measurement of the single coated HMTD sample shows a significantly stronger signal. The opening of the shutter can also be recognised here, whereby the signal is around 1.5 V. The signal then shows some irregularities, with smaller peaks of up to 0.7 V. The peaks that occur are presumably caused by smaller partial combustions in the sample, which do not lead to complete combustion of the sample. It can be seen that the occurrence of these peaks decreases with time. This can be caused by the removal of the graphite layer or the pushing of the graphite particles into the depth of the explosive sample. This trend continues in the measurements with a double graphite layer. The first impact of the laser on the sample is also clearly visible here. This is higher than in the other two measurements and is around 2.5 V. Here too, the signal tends to be rather irregular, which indicates a partial decomposition of the sample. One peak directly after opening the shutter and another at around 7 seconds are particularly noticeable. It can also be seen here that the occurrence and intensity of these peaks decrease with time.

Figure 4 shows exemplary measurements with all three coatings at 50 mW for TATP. The measurement without graphite shows, with the exception of the first impact of the laser, similar to HMTD, only very weak signals whose intensity remains constant over time and does not exceed 0.2 V. At the first impact of the laser, the signal is about 0.5 V high. The data show that the sample is processed without coating, but no significant partial conversion takes place. The measurement shown with a graphite coating shows more irregular peaks, which could be caused by partial conversions.The signals reach levels of up to 2 V. It can be seen that the intensity decreases with time, which is presumably caused by removing or pressing the graphite particles into the sample. If this is compared with the double-coated sample, it is noticeable that the latter has very strong peaks in the signal. The first impact of the laser is comparatively small in this measurement, but this is not the rule for these parameters. The signals sometimes exceed the microphone's dynamic range of 5 V. It is noticeable that the signal decreases sharply and almost falls to the level of the single-coated sample. This is also due to the removal of the graphite particles or the introduction of the graphite particles into the sample, which increases the absorption.

Exemplary measurements for sugar with 50 mW with all coating variations are shown in Figure 5. Looking at the measurement without graphite coating, the first impact of the laser on the sample with an amplitude of approximately 0.3 V is clearly recognisable. Otherwise, this measurement shows little deflection, which indicates that the sample is not or only very slightly processed. The signal does not exceed 0.1 V. If one compares the measurements with the simple graphite layer, significantly stronger signals can be seen. When the laser hits the sample for the first time, the signal reaches over 2.5 V. The subsequent signal curve shows many smaller peaks, which indicate processing. The peaks are smaller than with the explosives, which is due to the fact that the decomposition is not self-propagating and only small amounts of the sugar are decomposed. It is also noticeable that the signal intensities decrease with time, which indicates that the graphite particles are being driven into the sample or removed. Compared to the single-coated measurement, however, the signals are higher. When the laser strikes the graphite layer, a signal of just under 4 V is generated.

Figure 6 also shows some examples of data from samples where processing via laser led to complete combustion of the sample. As these would falsify the statistical analysis, these data were not taken into account. It is noticeable that when a sample is combusted, this happens in most cases directly after opening the shutter. This is probably due to the initially high amount of graphite which increases the formation of hot spots.

If one compares the exemplary measurements of all three substances in Figure 7, you can see that all substances show a clear signal. It can be seen that all samples also generate signals that exceed the dynamic range of the 5 V microphone. Over time, it is noticeable that the signal decreases for all samples. Compared to the other samples shown in this plot, the measurement of sugar shows fewer and also smaller peaks above the signal, which are caused by the decomposition of the sugar. The measurement with TATP shows high, narrow peaks over the entire measurement, whereby their frequency decreases over time. This is characteristic for measurements with TATP. It is also noticeable that a high basic low level of the signals can be recognised at the beginning of the measurement. This is due to partial redistribution of the material and a high availability of graphite at the beginning of the measurement. The observable partial combustion of the sample, as well as the general mechanism of decomposition, are probably triggered by hotspots, in which a graphite particle is heated by the strong absorption of the laser radiation and initiates the decomposition [23–25]. If this behaviour is compared with that

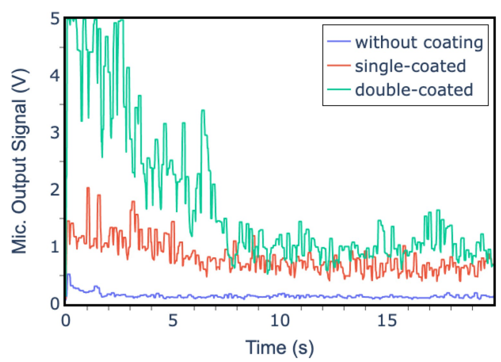

FIGURE 4 | Exemplary preprocessed microphone data of TATP – 50 mW – all coatings.

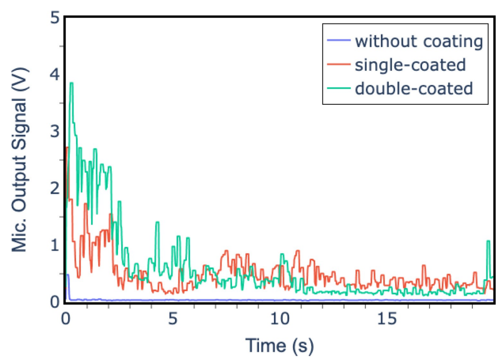

FIGURE 5 | Exemplary preprocessed microphone data of sugar – 50 mW – all coatings.

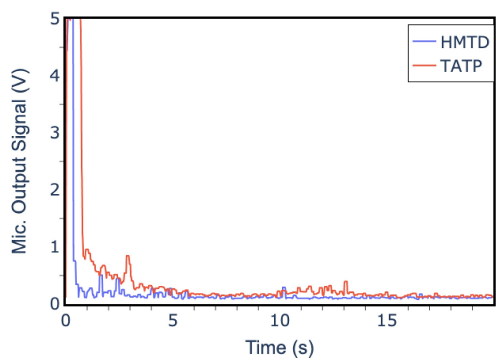

FIGURE 6 | Exemplary preprocessed microphone data of combusted samples —50 mW – double coated.

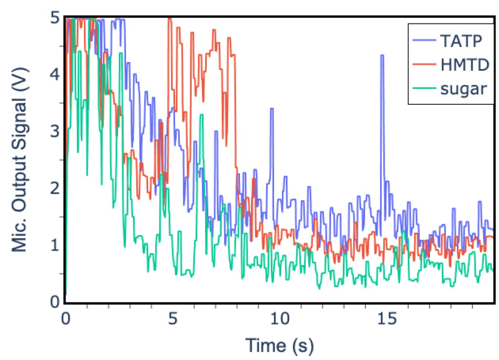

FIGURE 7 | Exemplary measurement for TATP, HMTD and sugar with single graphite coating at 100 mW.

of the HMTD sample, a high baseline of the signal can be seen here, particularly at the start of processing. This decreases in the course of the measurement. In contrast to TATP, HMTD shows a stronger accumulation of peaks during the measurement. It appears that the partial reactions are more intense here at the same laser power. This is also consistent with the observations that HMTD tends to react faster in the double-coated samples. In general, the microphone signal of the measurements with HMTD is not significantly higher than that of TATP, which may indicate that HMTD tends to react more strongly once a hotspot is created.

3.2.2 | Statistical Evaluation

In order to quantitatively analyze the data of the measurements, the data of all measurements with the same parameters (i. e. sample, reading and coating) were integrated and averaged over the groups. In the following, the data are shown in bar plots. Each plot represents the data of a substance at all powers and different coatings. The standard deviation is shown as an error bar.

Figure 8 shows the extracted integrals of the microphone data of all HMTD measurements. Looking at the mean values of the integrals over the different powers, it is clear to see that the amount of noise emissions generated by processing and partial decomposition increases with number of graphite layers applied. The uncoated sample shows a slight increase in the integral, with values increasing from 0.12 Vs at 12.5 mW to 0.31 Vs at 100 mW. It can be assumed that the values observed are dependent on the laser power. This is also shown by the HMTD measurements with a graphite layer. Here the values increase from 0.17 Vs at 12.5 mW to 1.42 Vs at 100 mW, too. Such an increase can also be seen in the measurements with two layers of graphite. The values here are approximately 0.19 Vs at 12.5 mW to 0.60 Vs at 25 mW. For future investigations, it could be determined whether there is an acoustic threshold above which a sample tends towards complete combustion.

Looking at the data situation for TATP (Figure 9), the picture is similar. Here, too, it is clear that the noise emissions increase with increasing power. The values 0.09 Vs at 12.5 mW rise to 0.35 Vs at 100 mW. It is noticeable that the values for TATP in the section are more power-dependent than those of the HMTD. This trend is also confirmed in the measurements with a single graphite layer. These range from 0.24 Vs at 12.5 mW to 2.04 Vs at 100 mW, which is higher than the value for HTMD. Looking at the plots for double coated samples, it can be seen that these are at 0.19 Vs at 12.5 mW and increase to 1.66 Vs at 50 mW. Again, this confirms the trend that the dependence of noise emissions on conductivity increases with increasing coating thickness. It is striking that the values of the single-coated samples at 12.5 and 25 mW are higher than those of the double-coated samples.

Looking at the statistically analysed data for sugar (Figure 10), there are differences to those for explosives. Basically, it can also be recognised here that the noise emissions increase with increasing laser power, but this is not as clear as with the explosives. For example, the emission of uncoated samples increases from 0.023 Vs at 12.5 mW to 0.045 Vs at 25 mW, but no further increase can be observed thereafter. However, both the single-coated sample and the double-coated sample with graphite show an increase. The values for single-coated samples and 12.5 mW range from 0.17 Vs to 1.4 Vs at 100 mW. What is striking about this substance is that the integrals of the signals for the single-coated sample are higher than those of the double-coated sample for three out of four lines. However, the differences are small compared to the differences between the single and double coated samples for the explosives, as can be seen from the standard deviations in the plots (TATP in Figure 9 and HMTD in Figure 8). The reason for this could be

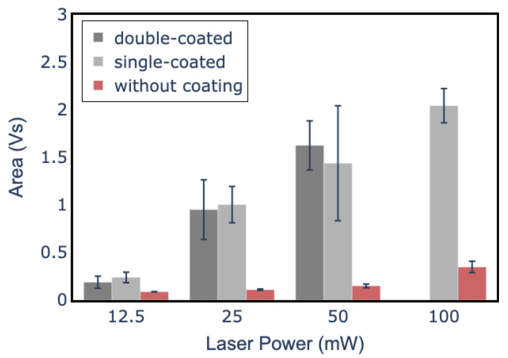

FIGURE 9 | Integral of the microphone signal of the TATP measurements averaged over all measurements with all coating types.

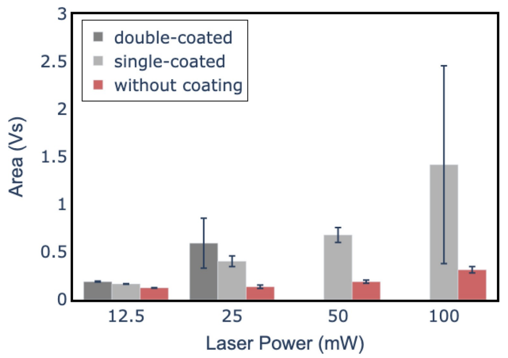

FIGURE 8 | Integral of the microphone signal of the HMTD measurements averaged over all measurements with all coating types.

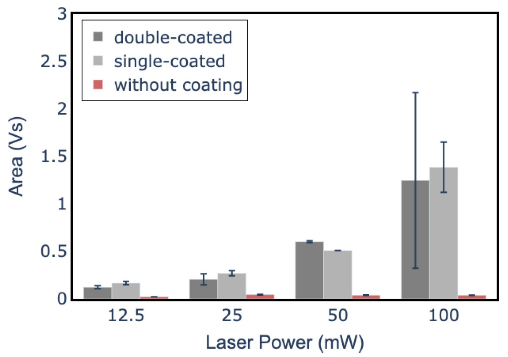

FIGURE 10 | Integral of the microphone signal of the sugar measurements averaged over all measurements with all coating types.

that the amount of graphite is relatively large and is not thrown out of the hole by smaller amounts, as could be the case with the explosives.

3.2.3 | Optical Evaluation

Figure 11 shows a single-coated TATP sample after treatment with 50 mW. The focus point of the laser is marked with a red cross. It can be seen that the processing has created a cavity. This has a diameter of about 600 μm. This is significantly larger than the beam diameter in the area where the laser hits the sample. The reason for this is that gas is produced during the processing of the sample, which flows out through the drill hole. This effect is intensified by the occurrence of small partial reactions that take place in explosives under laser irradiation. This observation is consistent with the fact that the intensity of the treatment decreases over time and that graphite is lost due to the partial over-expansion of the sample.

4 | Conclusion and Outlook

In this work we have analysed the behaviour of energetic materials under photonic irradiation. In experiments, HMTD, TATP and sugar with one, two and no graphite coatings were processed with a pulsed laser system at different power levels. The resulting acoustic signals were recorded and analysed using a MEMS microphone. On the one hand, the data show that the processing noise increases as expected with increasing power; this is basically independent of the material. It is noticeable that the increase in noise emissions as a function of power is dependent on the coating, particularly in the case of explosives. The processing noise per power increases the least without coating and the most with two coatings. The results suggest that the graphite particles increase the absorption of light and thus the energy absorption of the particles. This leads to an increase in the formation of hotspots [23, 24]. This in turn leads to partial conversion, which does not result in complete combustion of the sample, at least up to a certain value. The final threshold for HMTD is lower than that for TATP, which may indicate that HMTD, once initiated, is more likely to result in complete combustion than TATP. One reason for this could be the higher total specific energy release of HMTD, which favours a continuation of the reaction. This is 2.80 kJ/g for TATP and 5.08 kJ/g for HMTD [26].

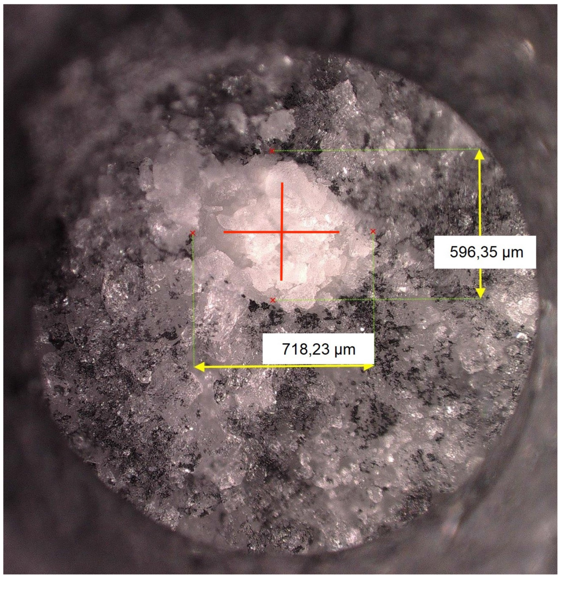

FIGURE 11 | Processed single-coated TATP sample,the focus point of the laser is marked with a red cross.

Another reason for this could be that different non-graphitized substances absorb light of different wavelengths to different degrees. In experiments with other wavelengths, the values could vary. The nature of the sample also plays a role. The reaction behaviour can vary due to grain sizes and geometries [24]. In the case of sugar, the influence of the graphite layer is significantly less. In particular, there is hardly any difference between single and double coating. It is also noticeable that the graphite is removed or particles are pushed into the sample over time. Another possibility is that the graphite is oxidised by the high energy input. This reduces the absorption of light over time and the colouration decreases. In particular, there is hardly any difference between single and double coating, the reason for this could be that with a layer of graphite there is already a kind of saturated layer. This means that the particles do not react so violently and also do not self-propagate, which means that fewer particles are transported away from the reaction zone, although some particles are still driven into the sample. One factor that can significantly influence the results is the quality of the layers. For the series of measurements carried out, the quality of the layers was checked under a microscope, and the results can vary due to irregularities and defects, as the surface of the samples is not completely flat despite pressing.

To summarize, the coating of samples combined with laser processing offers a method for decomposing or partially converting explosives in a more controlled manner and at lower power levels. Possibilities include both the targeted decomposition of substances and the transfer of decomposition products into the gas phase, as well as individual particles of the substance, and subsequent sampling for rapid identification of the substances. For future measurements, the substances should first be better characterised regarding particle size. A further step is to visualise the absolute optical sensitivities of the substances.

Acknowledgements

Open Access funding enabled and organized by Projekt DEAL.

Data Availability Statement

The data that support the findings of this study are available from the corresponding author upon reasonable request.

References

1. J. Oxley, J. Smith, W. Luo, and J. Brady, "Determining the Vapor Pressures of Diacetone Diperoxide (DADP) and Hexamethylene Triperoxide Diamine (HMTD)", *Propellants, Explosives, Pyrotechnics* 34 (2009): 539, https://doi.org/10.1002/prep.200800073.

2. J. C. Oxley, J. L. Smith, M. Porter, L. McLennan, K. Colizza, Y. Zeiri, R. Kosloff, and F. Dubnikov, "Synthesis and Degradation of Hexamethylene Triperoxide Diamine (HMTD)", *Propellants, Explosives, Pyrotechnics* 40 (2015): 644, DOI: 10.1002/prep.201500151.

3. A. Simon, and L. DeGreeff, "Variation in the Headspace of Bulk Hexamethylene Triperoxide Diamine (HMTD): Part II. Analysis of Non-Detonable Canine Training Aids", *Forensic Chemistry* 13 (2019): 100155, https://doi.org/10.1016/j.forc.2019.100155.

4. V. Bulatov, O. Reany, R. Grinko, I. Schechter, and E. Keinan, "Time-Resolved, Laser Initiated Detonation of TATP Supports the Previously Predicted Non-Redox Mechanism", *Physical Chemistry Chemical Physics* 15 (2013): 6041, https://doi.org/10.1039/c3cp44662j.

5. F. Dubnikova, R. Kosloff, Y. Zeiri, and Z. Karpas, "Novel Approach to the Detection of Triacetone Triperoxide (TATP): Its Structure and Its Complexes with Ions", *The Journal of Physical Chemistry A* 106 (2002): 4951, https://doi.org/10.1021/jp014189s.

6. W. Fan, M. Young, J. Caninoan, J. Smith, J. Oxley, and J. R. Almirall, "Fast Detection of Triacetone Triperoxide (TATP) from Headspace Using Planar Solid-Phase Microextraction (PSPME) Coupled to an IMS Detector", *Analytical and Bioanalytical Chemistry* 403 (2012): 401, https://doi.org/10.1007/s00216–012–5878-x.

7. S. Fan, J. Lai, P. L. Burn, and P. E. Shaw, "Solid-State Fluorescence-Based Sensing of TATP via Hydrogen Peroxide Detection", *ACS Sensors* 4 (2019): 134, https://doi.org/10.1021/acssensors.8b01029.

8. D. STANDARD, Moscheenanschlag in hernals: Selber sprengstoff wie in london verwendet, Available at: https://www.derstandard.at/story/2637639/moscheenanschlag-in-hernals-selber-sprengstoff-wie-in-london-verwendet2007, accessed: 13–11–2023.

9. G. Segell, "Terrorism on London Public Transport", *Defense & Security Analysis* 22 (2006): 45, https://doi.org/10.1080/14751790600577132.

10. Merkur, Sprengstoff-Brief an Gauck abgefangen, Available at: https://www.merkur.de/politik/sprengstoffverdaechtiger-brief-bundespraesidialamt-zr-2861520.html2023, accessed: 13–11–2023.

11. I. Dunayevskiy, A. Tsekoun, M. Prasanna, R. Go, and C. K. N. Patel, "High-Sensitivity Detection of Triacetone Triperoxide (TATP) and its Precursor Acetone", *Applied Optics* 46 (2007): 6397, https://doi.org/10.1364/AO.46.006397.

12. M. Amani, Y. Chu, K. L. Waterman, C. M. Hurley, M. J. Platek, and O. J. Gregory, "Detection of Triacetone Triperoxide (TATP) using a Thermodynamic Based Gas Sensor", *Sensors and Actuators B: Chemical* 162 (2012): 7, https://doi.org/10.1016/j.snb.2011.11.019.

13. X. Fang, and S. Ahmad, "Detection of explosive vapour using surface-enhanced Raman spectroscopy", *Applied Physics B* 97 (2009): 723, https://doi.org/10.1007/s00340–009–3644–3.

14. F. Zapata, M. López-López, and C. García-Ruiz, "Detection and identification of explosives by surface enhanced Raman scattering", *Applied Spectroscopy Reviews* 51 (2016): 227, https://doi.org/10.1080/05704928.2015.1118637.

15. A. M. Rodin, J. Sarlauskas, J. Tamuliene, A. Petrulėnas, Detection of Explosives by Ultrasonic Spectrum upon Pulsed Laser Initiation, in *Proceedings of SPIE Security + Defence, 2020, Counterterrorism, Crime Fighting, Forensics, and Surveillance Technologies IV*, volume 11542, SPIE 2020 page 115420E.

16. S. Wallin, A. Pettersson, H. Östmark, and A. Hobro, "Laser-based standoff detection of explosives: a critical review", *Analytical and Bioanalytical Chemistry* 395 (2009): 259, https://doi.org/10.1007/s00216–009–2844–3.

17. M. Bowden, Laser Initiation of Energetic Materials: A Historical Overview, in J. Thomes, F. Dickey (Editors), *Optical Technologies for Arming, Safing, Fuzing, and Firing III*, SPIE *Proceedings*, SPIE 2007 page 666208.

18. M. I. Sierra-Trillo, R. Thomann, I. Krossing, R. Hanselmann, R. Mülhaupt, Y. Thomann, "Laser Ablation on Isostatic Graphite—A New Way to Create Exfoliated Graphite", *Materials (Basel)* 2022, *15*, published online 2022 Aug 9.

19. J. C. Oxley, J. L. Smith, P. R. Bowden, and R. C. Rettinger, "Factors Influencing Triacetone Triperoxide (TATP) and Diacetone Diperoxide (DADP) Formation: Part I", *Propellants, Explosives, Pyrotechnics* 38 (2013): 244, https://doi.org/10.1002/prep.201200116.

20. J. C. Oxley, J. L. Smith, M. Porter, L. McLennan, K. Colizza, Y. Zeiri, R. Kosloff, F. Dubnikova, "Synthesis and Degradation of Hexamethylene Triperoxide Diamine (HMTD)," *Propellants, Explosives, Pyrotechnics* 41 (2016): 334, first published: 02 December 2015. https://doi.org/10.1002/prep.201500151.

21. A. Wierzbicki, E. A. Salter, E. A. Cioffi, and E. D. Stevens, "Density Functional Theory and X-ray Investigations of P- and M-Hexamethylene Triperoxide Diamine and Its Dialdehyde Derivative", *Journal of Physical Chemistry A* 105 (2001): 8763, https://doi.org/10.1021/jp0123841.

22. M. Muhr, T. Klapötke, G. Holl, "Sensory Monitoring of Drop Hammer Experiments with Multivariate Statistics", *Propellants, Explosives, Pyrotechnics* 47 (2022), DOI: 10.1002/prep.202200025.

23. T. M. Klapötke, *High Energy Materials* (Berlin, New York: Walter de Gruyter, 2009), ISBN: 978-3-11-020745-3, Pages: 233, URL: https://www.degruyter.com/document/doi/10.1515/9783110214888/html.

24. J. Köhler, R. Meyer, A. Homburg, *Explosivstoffe*, Wiley-VCH, Weinheim, 10th revised and expanded edition 2008, ISBN: 978-3-527-32009-7, Pages: 430, URL: https://www.wiley-vch.de/de/fachgebiete/naturwissenschaften/chemie-11ch/technische-u-industrielle-chemie-11ch3/explosiv-und-treibstoffe-11ch37/explosivstoffe-978-3-527-32009-7.

25. W. P. Bassett, B. P. Johnson, N. K. Neelakantan, and D. D. Dlott, "Shock Initiation of Explosives: High Temperature Hot Spots Explained", *Applied Physics Letters* 111 (2017): 061902, https://doi.org/10.1063/1.4985593.

26. A. Nazarian, and C. Presser, "Thermochemical analysis of improvised energetic materials by laser-heating calorimetry", *Thermochimica Acta* 707 (2022): 178971, DOI: 10.1016/j.tca.2022.178971.